Journal of Physiology (1990), **422**, *pp.* 303–320
With 10 figures
Printed in Great Britain

CALCIUM-DEPENDENT CHLORIDE CURRENT IN NEURONES OF THE RABBIT PELVIC PARASYMPATHETIC GANGLIA

BY T. AKASU, T. NISHIMURA AND T. TOKIMASA

From the Department of Physiology, Kurume University School of Medicine, 67 Asahi-machi, Kurume 830, Japan

(*Received 6 July 1989*)

SUMMARY

1. Voltage-clamp recordings were made from neurones in rabbit vesical pelvic ganglia by using single microelectrodes filled with 2 M-caesium chloride. Neurones were superfused with Krebs solution containing 300 nM-tetrodotoxin and 50 mM-tetraethylammonium.

2. Depolarizing voltage jumps activated inward currents followed by slowly decaying inward tail currents at −30 to +30 mV, which were accompanied by a large increase in membrane conductance. Both the inward current and tail current were blocked by cobalt (2 mM) or in a Krebs solution containing zero calcium and 12 mM-magnesium.

3. Substitution of barium for calcium enhanced the inward current, while it strongly reduced the tail current. Strontium substitution still exhibited both the inward current and the tail current.

4. Lowering external chloride activity increased the tail current amplitudes without affecting an initial calcium current. The reversal potentials of the tail current, measured using a twin-pulse protocol, were -18 ± 5 mV (mean ± S.E.M., $n = 8$) and $+5 \pm 3$ mV ($n = 5$) in Krebs solution and low-chloride (62 mM) solution, respectively, suggesting a calcium-dependent chloride current.

5. Stilbene derivatives, 4-acetamido-4′-isothiocyanostilbene-2,2′-disulphonic acid (SITS, 0·01–1 mM) and 4,4′-diisothiocyanostilbene-2,2′-disulphonic acid (DIDS, 0·01–1 mM), reversibly and concentration dependently depressed the tail current without affecting the calcium current.

6. Transient (T) and sustained (N and L) types of calcium current were likely to co-exist in neurones of the rabbit pelvic ganglia. Calcium-dependent chloride current was activated by N- and L-type calcium currents but not by T-type current.

7. Activation of the tail current at 0 to +20 mV was described by a single-exponential function. The tail current decayed exponentially at a holding membrane potential of −70 mV. Tail decay time constants were dependent on voltage and duration of the step command.

8. Substantial activation of the calcium-dependent chloride conductance could occur during a post-tetanic after-potential when pelvic ganglia neurones fired action potentials repetitively.

MS 7809

INTRODUCTION

Calcium-dependent chloride current (I_{Cl-Ca}) is widely distributed in a variety of excitable cells (Barish, 1983; Owen, Segal & Barker, 1984; Mayer, 1985; Korn & Weight, 1987; Rogawski, Inoue, Suzuki & Barker, 1988; Scott, McGuirk & Dolphin, 1988). Dorsal root ganglion (DRG) neurones in culture fire an action potential followed by an after-depolarization which corresponds to a slowly decaying inward tail current carried by chloride ions. This tail current is activated by elevation of intracellular calcium due to an activation of a calcium-induced calcium release mechanism (Barish, 1983; Miledi & Parker, 1984; Scott *et al.* 1988).

Recently, it has been reported that I_{Cl-Ca} is present in a large fraction of the trigeminal neurones but is observed only rarely in cultured parasympathetic neurones from quail embryo (Bader, Bertrand & Schlichter, 1987). Our previous current-clamp study has shown that the action potential with prolonged spike duration produced a calcium- and chloride-dependent spike after-depolarization when potassium conductance was blocked by application of tetraethylammonium and injection of caesium ions in parasympathetic neurones of the rabbit vesical pelvic ganglia (Tokimasa, Nishimura & Akasu, 1988*a*). This present study was designed to examine the characteristics and ionic mechanism of this spike after-depolarization. The results suggest that pelvic parasympathetic neurones of adult rabbits have a calcium-dependent chloride conductance and that substantial activation of the I_{Cl-Ca} occurred during repetitive firing of pelvic ganglia neurones and contributed to post-tetanic after-potentials. Preliminary accounts for some of this work have been published as abstracts (Tokimasa, Nishimura, Tsurusaki & Akasu, 1988*b*).

METHODS

Male white rabbits weighing 2·0–3·0 kg were anaesthetized with sodium pentobarbitone (40–50 mg kg^{-1} I.V.). Isolation of the vesical pelvic ganglia has been described previously (Nishimura, Tokimasa & Akasu, 1988). After removal of vesical pelvic ganglia, rabbits were killed by intravenous injection of an excess dose of pentobarbitone. Connective tissue surrounding the ganglia was removed as much as possible by dissection, so that the cells were much easier to penetrate and easier to expose with applied solutions. Individual ganglia were then pinned onto Sylgard at the bottom of a perfusion chamber and continuously superfused with Krebs solution having the following composition (mM): NaCl, 117; KCl, 4·7; $CaCl_2$, 2·5; $MgCl_2$, 1·2; NaH_2PO_4, 1·2; $NaHCO_3$, 25 and glucose, 11. The solution was gassed with 5% CO_2–95% O_2 and preheated to 35–37 °C at the recording site.

Electrophysiological experiments

Voltage and current recordings were made with the Axoclamp 2A (Axon Instruments, Burlingame, CA, USA). For current-clamp experiments, ganglion cells were impaled with glass microelectrodes filled with 3 M-potassium chloride or 2 M-caesium chloride and had tip resistances of 30–50 MΩ. Current injection was made through a recording microelectrode. For discontinuous single-electrode voltage clamp, glass microelectrodes were filled with 2 M-caesium chloride with tip resistances of 20–40 MΩ. Sampling frequency was between 3 and 5 kHz with a 70–30 duty cycle. The head stage of the amplifier was monitored on a separate oscilloscope. The signal from the microelectrode was displayed on an oscilloscope with digitized memory (Nihon Kohden, VC-11) and recorded on a penwriting chart recorder.

Leak currents were determined by applying hyperpolarizing voltage commands of magnitudes

equal to the depolarizing command used to evoke the inward current. Alternatively, leak currents were also recorded during depolarizing commands equivalent to those used to evoke inward currents after block of calcium currents by cobalt (1–2 mM) or by removal of calcium (or barium) from the superfusing solution containing 12 mM-magnesium. In either case, leak currents were subtracted from the relevant inward currents to yield the calcium (or barium) currents.

Solutions

To record inward calcium and chloride currents, the superfusing solution routinely contained 300 nM-tetrodotoxin (TTX) and 50 mM-tetraethylammonium (TEA) chloride, where NaCl was reduced to 67 mM. Application of TEA to extracellular space and the intracellular injection of caesium ions almost completely depresses potassium conductance present on neurones in the rabbit vesical pelvic ganglia (Nishimura *et al.* 1988). In some experiments, calcium was replaced with equimolar barium or strontium. Low-chloride solution was made by replacement of 67 mM-chloride with equimolar isethionate. Sucrose-Krebs solution contains (mM): sucrose, 234; KCl, 4·7; $MgCl_2$, 1·2; NaH_2PO_4, 1·2; $NaHCO_3$, 25 and glucose, 11. Calcium-free solution contains zero calcium and 12 mM-magnesium. Solutions for voltage-clamp experiments routinely contained 1 mM-caesium chloride to depress an anomalous rectification (Nishimura *et al.* 1988).

Drugs

Drugs used were tetrodotoxin (TTX) from Sankyo; tetraethylammonium chloride (TEA) from Tokyo Kasei (Japan); 4-acetamido-4′-isothiocyanostilbene-2,2′-disulphonic acid, disodium $3H_2O$ (SITS) from Research Organics (USA); 4,4′-diisothiocyanostilbene-2,2′-disulphonic acid, disodium salt (DIDS), from Dojindo Laboratories (Kumamoto, Japan); ω-conotoxin GVIA from Peptide Institute (Osaka); (+)-tubocurarine hydrochloride and apamin from Sigma.

Numerical expressions are mean ± S.E. of the mean.

RESULTS

Inward current and tail current

Neurones ($n = 95$) of the rabbit vesical pelvic ganglia superfused with a solution containing 300 nM-TTX and 50 mM-TEA were impaled with intracellular microelectrodes filled with CsCl. After injection of caesium ions by cathodal DC (0·3–0·7 nA for 5–10 min), the resting membrane potentials were between −35 and −10 mV. Membrane potential was maintained more negative than −50 mV. Under these conditions, brief depolarizing pulses (2–20 ms duration) produced action potentials with prolonged spike repolarization followed by a depolarizing after-potential (Fig. 1*A*) (Tokimasa *et al.* 1988*a*).

The ganglion neurones were then voltage clamped at a holding membrane potential of −50 to −100 mV to examine the ionic mechanism of the depolarizing after-potential. Figure 1*B* shows typical current responses of pelvic ganglia neurones by hyperpolarizing and depolarizing voltage jumps from a holding potential of −70 mV to potentials of −90 to +30 mV. Depolarizing voltage steps produced inward currents followed by slowly decaying inward tail current in 97% ($n = 92$) of the neurones tested (Fig. 1*B*). During the voltage jumps to potentials around −15 mV, net inward current occurred with a slow inward relaxation, while further depolarization to +30 mV causes a slow outward relaxation of a net outward current. Under this condition, since outward-going potassium conductance was nominally depressed due to internal caesium ions and external TEA (Nishimura *et al.* 1988; Tokimasa *et al.* 1988*a*), some conductance mechanism other than voltage-

and/or calcium-dependent potassium currents underlies the time-dependent outward current. Depolarization to a more positive membrane potential than +30 mV strongly reduced the amplitude of the tail current (Fig. 1*B*).

These two inward currents seemed to be attributed to activation of different

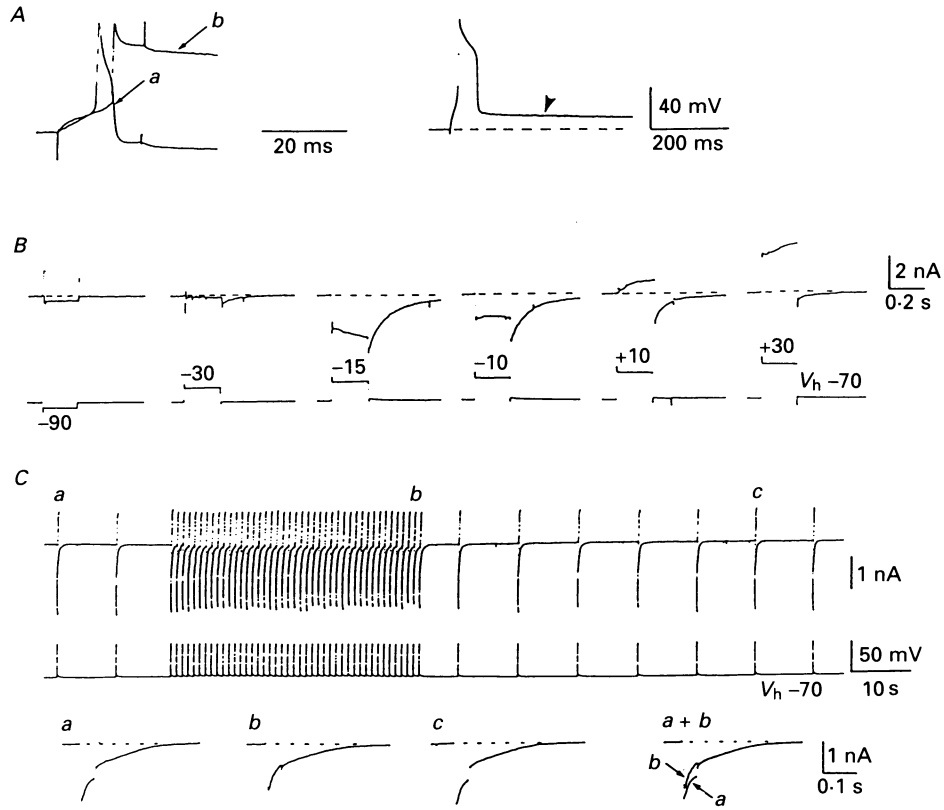

Fig. 1. Voltage and current responses recorded from neurones in rabbit pelvic ganglia. *A*, action potentials were elicited by passing depolarizing current pulses (0·3 nA for 20 ms) through the recording microelectrode. The resting membrane potential was maintained at −54 mV by passing hyperpolarizing DC (0·5 nA). In the left traces, action potentials obtained before (*a*) and 5 min after caesium injection (*b*) were superimposed. Record *b* is also shown in the right trace where time scale is reduced. Arrow-head indicates depolarizing after-potential. *B*, typical current responses evoked by voltage jumps to potentials −90 to +30 mV from holding potential (V_h) of −70 mV. Caesium was injected into the ganglion cell superfused by Krebs solution containing 300 nM-TTX and 50 mM-TEA. Note that inward calcium current (I_{Ca}) was followed by an inward tail current. *C*, I_{Ca} and tail current evoked by voltage jumps from −70 to −20 mV at frequencies of 0·1 Hz and 1 Hz. Lower traces *a*–*c* are expanded records of these currents which correspond to the time marked by the respective letters in the upper trace. Note that the amplitude of the I_{Ca} showed 'run-down' when evoked at 1 Hz for 40 s, where the tail current is not altered. Data for *A*, *B* and *C* were obtained from three different cells.

conductance systems. Stable recordings of both initial inward calcium current and tail current with constant amplitudes could be made by repeated application of depolarizing step commands (50 ms duration) at a rate of 0·1 Hz (Fig. 1*C*). When the frequency was increased to 1 Hz, the inward current appeared to decrease in

amplitude with time, while the tail current remained almost unchanged ($n = 3$) (Fig. 1*C*). The 'run-down' of the initial inward current may result from an inactivation of calcium channels caused by increased intracellular calcium (Brehm & Eckert, 1978; Tillotson, 1979; Hille 1984).

Current–voltage relationships of inward current and tail current

Both inward current and tail current were a function of membrane potential. Figure 2*A* shows examples of current–voltage (*I–V*) plots of these currents obtained from a single neurone using voltage commands of 200 ms in duration. Peak inward current occurred around −15 mV (mean -15 ± 1 mV, $n = 22$). Depolarization beyond this potential by voltage jumps produced net outward currents with outward relaxation; the inward current measured at the end of command pulses reversed polarity at −10 to +15 mV. On the other hand, an instantaneous *I–V* plot of the inward current recorded at the beginning of command pulses showed a reversal around +3 to +38 mV (see also Fig. 3*Ba*). This difference reflects time-dependent activation of an outward current at depolarized membrane potentials. In these neurones, plots of inward tail current amplitude recorded at −70 mV provided a U-shaped *I–V* curve with a peak between −25 and +10 mV (-11 ± 2 mV, $n = 22$), similar to the membrane potential at which the peak of initial inward current is recorded (Fig. 2*A*). The amplitude of tail currents was $2{\cdot}6 \pm 0{\cdot}5$ nA ($n = 22$). Depolarization to more positive membrane potentials strongly reduced the amplitude of the tail current, presumably because of a decreased driving force for calcium ions (see following section).

Calcium dependence of inward current and tail current

The calcium-dependent mechanism underlying the tail current was examined by changing the extracellular medium for calcium-free 12 mM-magnesium solution (Fig. 2*A*). This reversibly abolished the inward current activated during depolarizing voltage jumps, resulting in a more linear current–voltage relation over the range −100 to +40 mV (Fig. 2*A*). Inward tail current was also dramatically reduced in calcium-free solution (Fig. 2*A*). A similar and reversible depression of these currents occurred during application of cobalt (1–2 mM, $n = 5$) (Fig. 2*B*). In the presence of cobalt (1 mM), the current–voltage curve became almost linear, providing further evidence that the tail current is largely dependent on a prior or simultaneous calcium entry.

Specificity of divalent cations for the tail current

Barium substitution for calcium

Ability of other divalent cations to produce the tail current was examined in neurones of pelvic parasympathetic ganglia. Barium-induced inward current (I_{Ba}) had a larger amplitude than that of inward calcium current (I_{Ca}) at −10 mV (Figs 3 and 5*A*). The I_{Ba} was blocked by 1 mM-cobalt, suggesting that barium ions can pass through calcium channels as charge carriers. However, barium produced only a small inward tail current which was less than 20% ($n = 10$) of the tail current obtained in calcium (2·5 mM)-containing solution (Fig. 3*A*). Simple addition of barium (2·5 mM) to calcium (2·5 mM)-containing solution produced no blockade of the tail current

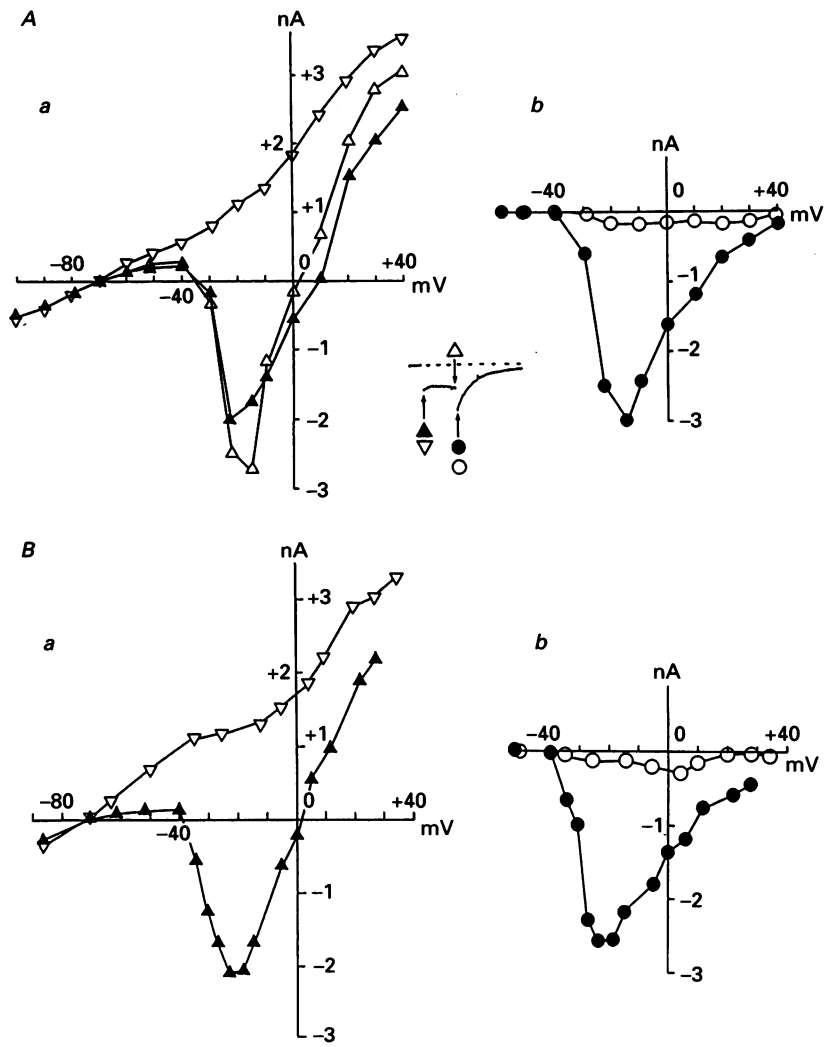

Fig. 2. Calcium dependence of the current–voltage (I–V) curve for I_{Ca} (a) and a I–V curve of the tail current (b). A, blockade of I_{Ca} and tail current in Ca^{2+}-free solution. In inset, ▲ and △ represent the inward currents measured at the beginning and the end of depolarizing command pulses, respectively. ▽ in graph a represents instantaneous current–voltage curve obtained in Ca^{2+}-free solution. ● and ○ in graph b represent results obtained in Krebs solution and Ca^{2+}-free solution, respectively. B, blockade by 1 mM-cobalt ions. ● and ○ represent results obtained in Krebs solution and cobalt (1 mM)-containing solution, respectively. ▽ indicates current–voltage curve obtained in the presence of cobalt (1 mM). Note that when the I_{Ca} is blocked by the removal of calcium ions or the addition of cobalt ions, the tail current is also strongly reduced. Data in graphs A and B were obtained from different cells.

($n = 3$). Figure 3B shows examples of current–voltage plots of I_{Ca}, I_{Ba} and the tail current obtained from a single ganglion neurone, measured using voltage commands 100 ms in duration. Peak inward current of I_{Ba} occurred at around -10 mV (-12 ± 3 mV, $n = 3$), similar to those for I_{Ca}. The potential which inverses the net

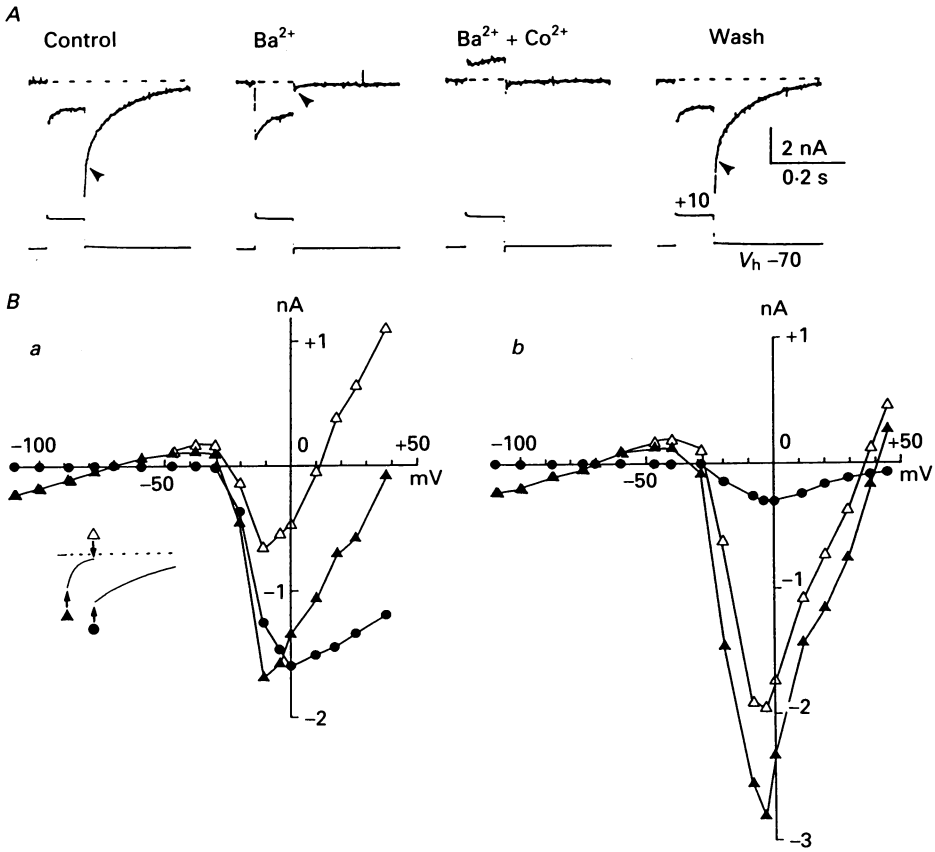

Fig. 3. Suppression of the tail current by substitution of barium for calcium. *A*, 2·5 mM-calcium was replaced by equimolar barium. Cobalt (1 mM) was added to barium-containing solution. Arrow-heads indicate the tail current. *B*, current–voltage curves of the inward currents (▲, △) and the current–voltage curve of the tail current (●). Inset shows the I_{Ca} and the tail current. In graph *a*, ▲ and △ represent I_{Ca} measured at the beginning and end of command pulses, respectively. Graphs *a* and *b* were obtained from the same cell in Krebs solution and barium solution, respectively. Data in *A* and *B* were obtained from different cells.

current was $+28 \pm 5$ mV ($n = 3$) for I_{Ba}. No obvious tail current was evoked at all holding potentials tested (Fig. 3*Bb*).

Strontium substitution for calcium

Substitution of strontium (2·5 mM) for calcium also exhibited an inward current (I_{Sr}) with slower decay than that of I_{Ca} during depolarizing voltage jumps. The I_{Sr} appeared to be followed by an inward tail current ($n = 5$) (Fig. 4*A*). Figure 4*B* also shows examples of *I–V* relationships for I_{Sr} and the tail currents obtained from a pelvic ganglion neurone. Strontium did not change the voltage dependence of the calcium conductance. Characteristics of this strontium-induced tail current were essentially the same as those of the tail current induced by calcium. The peak

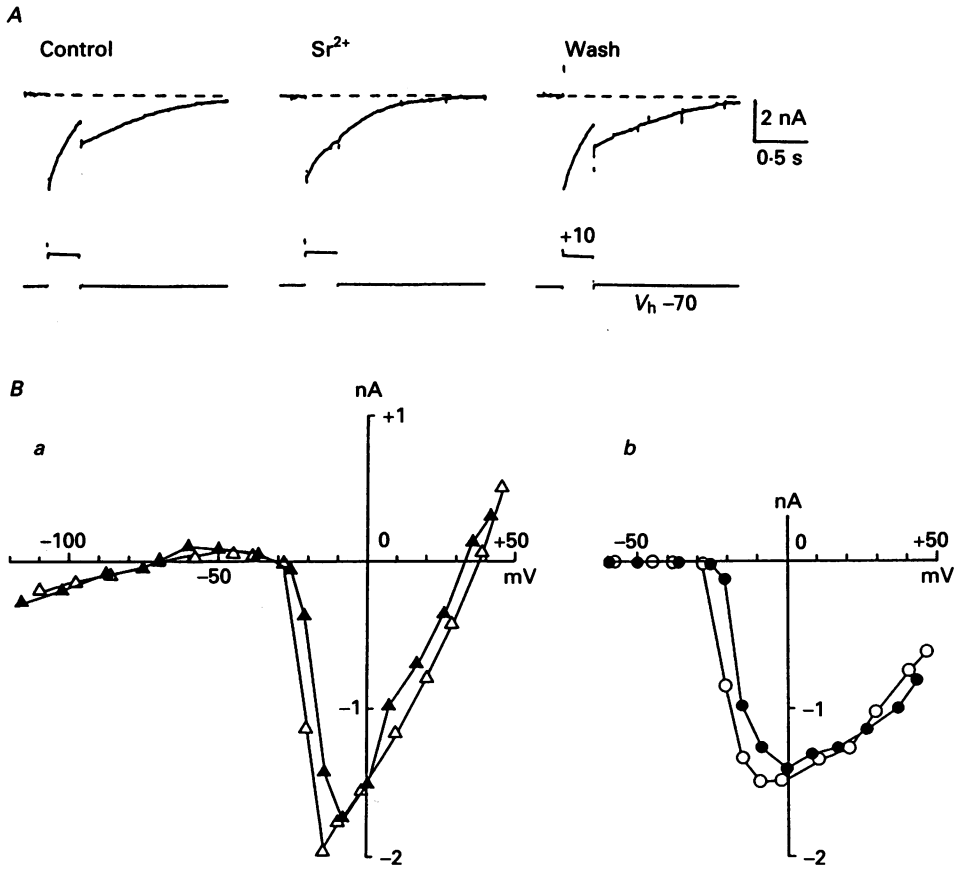

Fig. 4. Substitution of equimolar strontium for calcium. *A*, left and middle traces were obtained before and 5 min after replacement of calcium by strontium (2·5 mM), respectively. Right trace was obtained 5 min after washing of the pelvic ganglion neurone with strontium-free Krebs solution. *B*, the instantaneous current–voltage curve of strontium current (*a*) and the current–voltage curve of the tail current (*b*). Filled and open symbols represent the inward currents obtained in Krebs solution and strontium solution, respectively. Note that the strontium inward current was followed by the tail current. Data in *A* and *B* were obtained from two different cells.

amplitudes of I_{Sr}, 1·5–3 nA, and of the tail current, 2–3 nA, occurred around −10 mV in strontium medium ($n = 3$).

Membrane conductance change and reversal potential of the tail current

Changes in membrane conductance were measured during these inward currents by using hyperpolarizing step commands of 50 ms in duration. The membrane conductance was markedly increased during the tail current (Fig. 5*A*). Mean conductance increase was 16–70 nS (36 ± 8 nS, $n = 6$) at the peak of the tail current. When 1 s voltage jumps from −75 to −20 mV were applied to activate the inward current, the initial negative slope conductance was converted to a positive slope

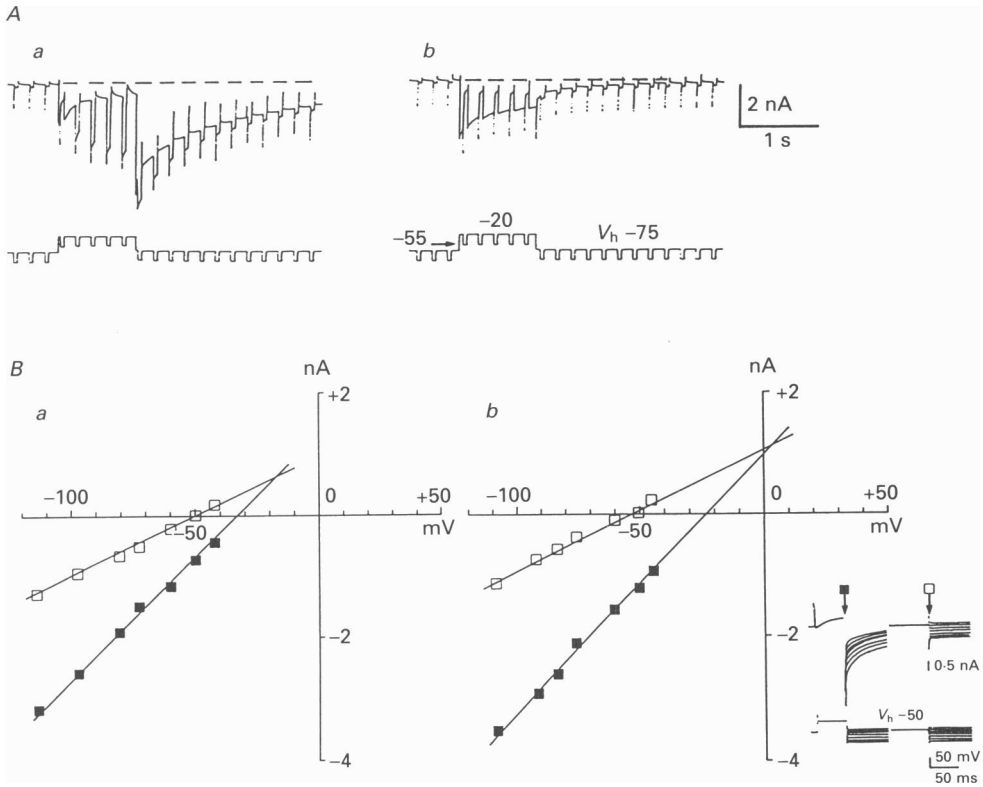

Fig. 5. Conductance changes during the inward currents and the tail current (*A*) and the reversal potential of the tail current (*B*). *A*, inward currents were evoked by a depolarizing command pulse (1 s duration) from −70 to −20 mV. Hyperpolarizing command pulses with an amplitude of 35 mV and 50 ms duration were superimposed on the depolarizing command at a rate of 5 Hz. Record *a* was obtained in Krebs solution containing 2·5 mM-calcium. Record *b* was obtained in a solution where calcium was totally replaced with barium. *B*, extrapolated reversal potentials of the tail current obtained by using twin-pulse (inset) protocol. ■ and □ indicate the amplitude of the tail currents and the leak currents, respectively. The neurone was initially held at −50 mV. Data in graphs *a* and *b* were obtained in Krebs solution and in low-Cl^- (62 mM) solution, respectively.

which developed during the inward current. At −20 mV, activation of the conductance mechanism occurred as a slow outward relaxation; the envelope of the conductance-testing pulses at −55 mV was seen as a slow inward relaxation. Such a development of the positive slope conductance implies an activation of chloride current by inward calcium currents (Mayer, 1985). The envelope experiments provided a reversal of the tail current of -20 ± 7 mV ($n = 6$). When extracellular calcium was replaced by barium, the tail current disappeared and only negative slope conductance was observed during I_{Ba} (Fig. 5*Ab*).

A two-step voltage-clamp method was used to estimate the reversal potential of the tail current (Fig. 5*B*). The current–voltage relation at the peak of the tail current was linear over the potential range −120 to −40 mV, giving an extrapolated

reversal potential of -18 ± 3 mV ($n = 8$). The reversal potential of the tail current was also obtained in a low-chloride solution, where 67 mM-chloride was replaced with equimolar isethionate. The extrapolated reversal potential of the tail current from the I–V curve was $+5\pm3$ mV ($n = 5$) in low-chloride solution (Fig. 5*B*).

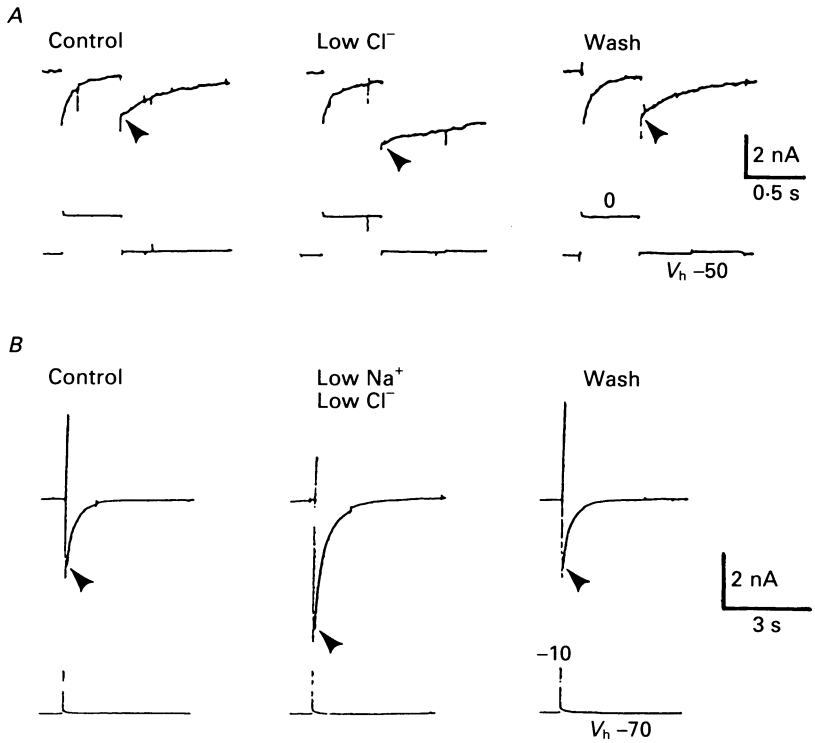

Fig. 6. Chloride dependence of the tail currents. *A*, replacement of 67 mM-NaCl with equimolar sodium isethionate. The tail currents were evoked by voltage jumps from −50 to 0 mV for 500 ms. *B*, substitution of 234 mM-sucrose for 117 mM-NaCl. The solution did not contain TEA. The tail currents were evoked by voltage jumps from −70 to −10 mV for 50 ms. Arrow-heads indicate peak of the tail current. Records *A* and *B* were obtained from two different cells.

Chloride dependence of the tail current

Recent reports have shown that a calcium-dependent tail current was carried by chloride ions (Mayer, 1985; Bader *et al.* 1987; Korn & Weight, 1987). Reduction of extracellular chloride ions to 62 mM by replacement with isethionate markedly augmented the amplitude of the tail current, while it produced no increase in the peak amplitude of the inward calcium current (Fig. 6*A*). The facilitation of the tail current was presumably as a result of an increased driving force for chloride ions.

Activation of non-selective cation-permeable channels also has been reported to contribute to the generation of inward current tails dependent on calcium entry (Colquhoun, Neher, Reuter & Stevens, 1981; Partridge & Swandulla, 1988). To test the possibility that sodium ions are also charge carriers which produce the inward tails in neurones of pelvic ganglia, the superfusing solution was switched from

standard Krebs solution to a sucrose-Krebs solution where 117 mM-NaCl was totally replaced with sucrose. Under this condition, the amplitude of the tail current was increased ($n = 3$) (Fig. 6*B*). Simple removal of sodium (117 mM) by replacement of sodium chloride with equimolar choline chloride did not alter the tail current ($n = 3$). These results suggest that the inward tail current is mostly carried by chloride ions.

Effects of chloride channel blockers on the tail current

The involvement of an anion-dependent mechanism in a calcium-dependent inward tail current was investigated using SITS and DIDS. These stilbene derivatives have been reported to block voltage-gated chloride currents in the squid axon (Inoue, 1985), skeletal muscle (Bretag, 1987), cultured rat astrocytes (Gray & Ritchie, 1986), sensory neurones (Bader *et al.* 1987) and endocrine cells (Korn & Weight, 1987). SITS (1 mM) strongly suppressed the tail current, while it caused almost no change in the inward calcium current (Fig. 7*A*). This effect occurred in about 1 min after beginning its application. The inhibition of the tail current was dependent on the concentration of SITS (Fig. 7*B*). Figure 7*Ca* shows a current–voltage relation for the tail current obtained at a holding voltage stepped from −70 to −90 mV through +25 mV in the absence or presence of SITS (100 μM). Another stilbene derivative, DIDS (10 μM–1 mM), produced a similar depression of the tail current evoked at −35 to +20 mV, without producing a blockade of the calcium current (Fig. 7*Cb*). The effects of both SITS and DIDS were readily reversible; depression of the tail current recovered within 10 min after removal of these drugs.

Transient and sustained calcium currents for I_{Cl-Ca}

According to Nowycky, Fox & Tsien (1985), three types (T-, N- and L-type) of calcium currents can be observed in DRG neurones from the chick embryo. Transient and sustained barium currents could also be recorded from neurones in pelvic ganglia, where barium was substituted for calcium to avoid a contamination of chloride current during the inward current. In about 40% of the neurones tested, depolarizing voltage commands applied from −100 to −50 mV produced an inward barium current with rapid inactivation (Fig. 8*A*). Amplitude and decay time constants of the transient current are $0{\cdot}4 \pm 0{\cdot}2$ nA ($n = 3$) and 20 ± 3 ms ($n = 3$), respectively. This rapidly inactivating current may correspond to the T-type current (Nowycky *et al.* 1985; Fox, Nowycky & Tsien, 1987). When the membrane potential was held at −60 mV, where T-type current is assumed to be inactivated (Nowycky *et al.* 1985), a depolarizing voltage command with duration of 200 ms produced an inward current associated with no transient component of calcium current at −10 mV (Fig. 8*A*). A sustained inward current was $3 \pm 0{\cdot}3$ nA ($n = 5$) at −10 mV and decayed with a double-exponential function; the time constants for fast and slow components were 150 ± 40 ms ($n = 5$) and 560 ± 110 ms ($n = 5$), respectively. ω-Conotoxin has been reported to block irreversibly N- and L-type currents (McCleskey, Fox, Feldman, Cruz, Olivera, Tsien & Yoshikami, 1987). The sustained current in pelvic ganglion cells was also strongly but reversibly suppressed by ω-conotoxin (500 nM, Fig. 8*B*). The L-type current was separated from the sustained current. In pelvic ganglion cells, the membrane potential was initially held at −40 mV, where N-type current is assumed to be strongly inactivated (Nowycky *et al.* 1985; Fox *et al.*

1987). Under this condition, voltage jumps applied to −10 mV produced a long-lasting barium current with an amplitude of 0·2–0·6 nA. The L-type current showed a 'run-down' at −40 mV, when voltage jump was applied at an interval of 10–30 s.

T-type calcium current was not followed by a clear tail current (Fig. 8*Ca*). On the

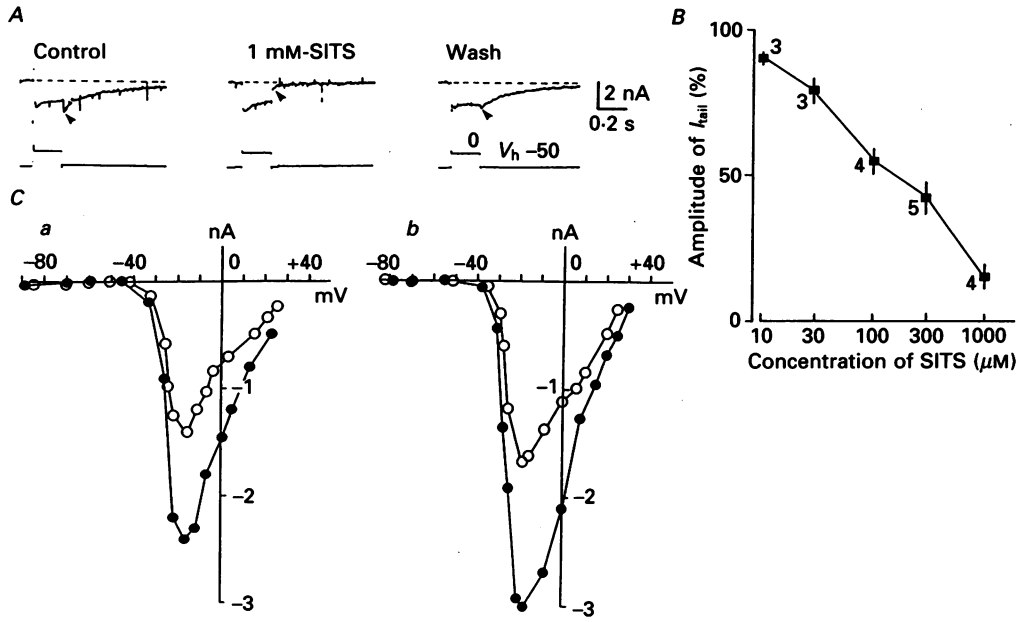

Fig. 7. Blockade of the tail current by chloride channel blockers. *A*, effects of 1 mM-SITS on the I_{Ca} and the tail current. Left and middle traces were recorded before and 5 min after application of the agent, respectively. Right record was taken 10 min after removal of SITS. Arrow-heads indicate the tail current. *B*, dose–responses curve for SITS effects on the tail current. Number of cells tested is shown at each point. Vertical bars indicate standard error of mean. *C*, effects of 300 μM-SITS (*a*) and 100 μM-DIDS (*b*) on the current–voltage curve of the tail current. ● and ○ represent data obtained before and 5 min after the application of agents, respectively.

other hand, sustained current obtained by a voltage jump from −60 to −20 mV appeared to activate a large inward tail current (Fig. 8*Cb*). Isolated L-type calcium current was also followed by the tail current (Fig. 8*Cc*). The tail current was strongly reduced by ω-conotoxin (500 nM) (Fig. 8*D*), suggesting that L- and N-type, but not T-type, currents can activate the chloride current in pelvic parasympathetic neurones.

Activation and deactivation kinetics of $I_{Cl\text{-}Ca}$

Amplitudes of the tail current recorded on repolarization to −60 mV were plotted as a function of duration of a depolarizing pre-pulse to activate $I_{Cl\text{-}Ca}$. The tail current increased as the duration of the voltage jump was increased (Fig. 9*A*). Activation of $I_{Cl\text{-}Ca}$ at 0 to +10 mV was described by a single-exponential function of time constant 170–500 ms (mean 350±150 ms, $n = 3$). During a prolonged depolarizing voltage jump, the tail current did not show appreciable inactivation (Fig. 9*A*).

At −55 mV, the tail current activated by depolarizing pre-pulses of duration 200–600 ms decayed as a single-exponential function of time constant 0·2–1·2 s. The decay time constant increased as a function of the duration of the pre-pulse (Fig. 9*B*). However, using depolarizing commands with duration longer than 1 s, the tail

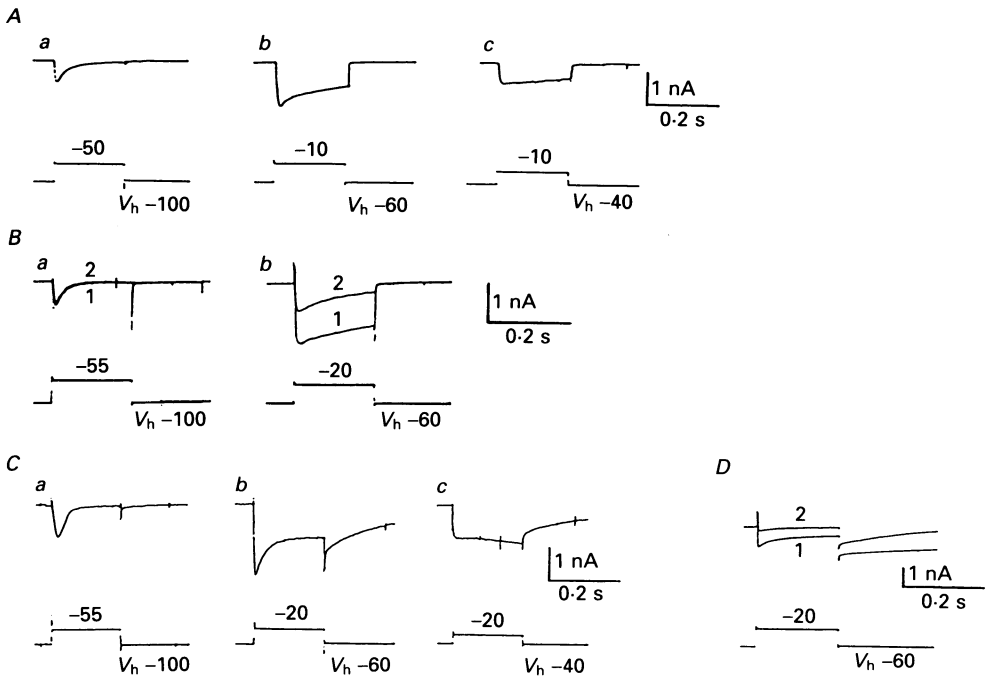

Fig. 8. *A*, transient and sustained barium currents (I_{Ba}) in neurones of pelvic ganglia. Equimolar barium was substituted for calcium in the superfusing solution. T-current (*a*) was obtained by voltage jump from a holding potential of −100 to −50 mV. Sustained current (*b*) evoked at −10 mV from a holding potential of −60 mV. L-current was evoked at −10 mV from a holding potential of −40 mV. Records *a*, *b* and *c* were obtained from the same neurone. *B*, effect of ω-conotoxin (500 nM) on the transient and sustained I_{Ba}. Records 1 and 2 were taken before and 3 min after application of ω-conotoxin. Records *a* and *b* were obtained from the same neurone. Note that ω-conotoxin selectively blocked the sustained current. *C*, tail currents produced by I_{Ca}. Methods for isolation of transient (*a*) and sustained (*b* and *c*) I_{Ca} were the same as those for barium currents. Records *a*, *b* and *c* were obtained from the same neurone. Note that sustained current but not transient current activate tail currents. Leak currents were subtracted (see Methods). *D*, inhibition of the tail current by ω-conotoxin (500 nM). Records 1 and 2 represent I_{Ca} recorded before and 3 min after application of ω-conotoxin, respectively. Records *A–D* were obtained from four different cells.

current kinetics were no longer described by a single-exponential function. The decay of the tail current was also dependent on the membrane potential; it became faster with hyperpolarization over the range −40 to −100 mV (Fig. 9*C* and *D*).

Contribution of I_{Cl-Ca} to post-tetanic after-potential

Contribution of I_{Cl-Ca} to the action potential was examined on neurones in pelvic ganglia by using KCl electrodes. A single action potential evoked by direct

stimulation was followed by an after-hyperpolarization (AHP), lasting up to 55 s (10 ± 2 s, $n = 50$) in neurones of pelvic ganglia superfused with the Krebs solution (Nishimura *et al.* 1988). When a train of repetitive depolarizing currents (20 Hz for 2 s) was applied to the ganglion cells, a burst of action potentials was followed by a

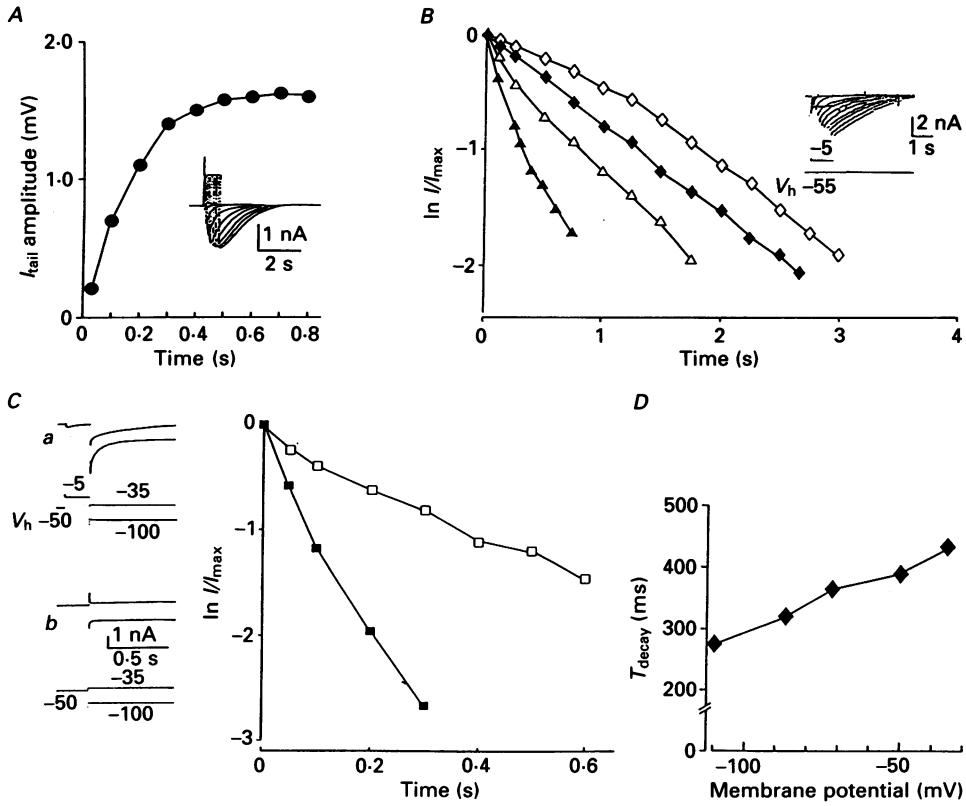

Fig. 9. Activation and deactivation kinetics of the tail current. *A*, plot of the tail current amplitude (inset) *versus* the duration of depolarizing voltage commands to 0 mV from −50 mV. *B*, decay of the tail currents plotted on a semilogarithmic scale against time. Lines through points were fitted by interpolation. Tail currents were evoked by depolarizing voltage jumps with a duration of 0·2–1 s (◇), 1·0 s; (◆), 0·6 s; (△), 0·4 s; (▲), 0·2 s. *C*, semilogarithmic plots of the tail current decay recorded at −35 (□) and −100 mV (■). Depolarizing pre-pulse (200 ms) was applied from −50 to −5 mV. The inset shows the raw data of the experiment. Traces *a* and *b* represent tail currents and leak currents, respectively. Each amplitude of the tail current was obtained by subtraction of the leak current from the tail current traces. *D*, plots of the time constant (τ) for the tail current *versus* membrane potentials. Records *A–D* were obtained from different cells.

hyperpolarizing after-potential, post-tetanic hyperpolarization (PTH). Figure 10*A* shows examples of the AHP and PTH recorded from the same ganglion cell. Interestingly, the duration of the PTH was shorter than that of the AHPs in most neurones tested (Fig. 10*A*). The mean duration of the PTH elicited by depolarizing current pulses (20 Hz, 2 s) was $2{\cdot}2 \pm 0{\cdot}2$ s ($n = 7$).

It has been reported that (+)-tubocurarine (curare) inhibits the calcium-activated

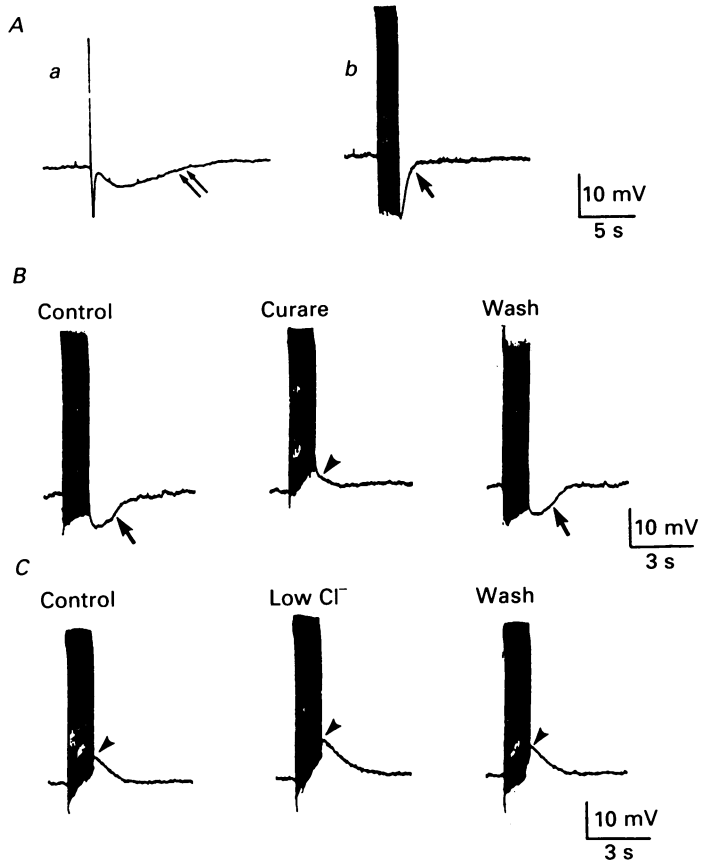

Fig. 10. Activation of $G_{Cl\text{-}Ca}$ during post-tetanic hyperpolarization and depolarization in pelvic ganglia neurones. *A*, spike after-hyperpolarization (*a*) was evoked by a single action potential (↑↑). The post-tetanic hyperpolarization (*b*) was evoked by a train of action potentials, 20 Hz for 3 s (↑). Action potentials were evoked by injection of depolarizing current pulses of 0·8 nA for 4 ms. Records *a* and *b* were obtained from the same pelvic ganglion neurone. Note that the duration of the single after-hyperpolarization is longer than that of post-tetanic hyperpolarization. *B*, effect of curare on the post-tetanic hyperpolarization. Left and middle traces were obtained before and 5 min after the application of 300 μM-curare, respectively. Right trace was obtained 10 min after removal of curare from the perfusate. Note that the post-tetanic hyperpolarization (↑) was converted to the post-tetanic depolarization (▼) in the presence of curare. *C*, chloride dependence of the post-tetanic depolarization in solution containing 300 μM-curare. The post-tetanic depolarization was augmented when 67 mM-chloride was replaced by equimolar isethionate.

potassium conductance ($G_{K\text{-}Ca}$) in neurones of the rabbit pelvic ganglia (Nishimura *et al.* 1988). Application of curare (300 μM) to the ganglion cells caused a strong suppression of the PTH; the PTH was converted to a depolarizing after-potential (post-tetanic depolarization, PTD) during repetitive firing of the action potential. Apamin (10–100 nM), reported to be a potent blocker for $G_{K\text{-}Ca}$ in neurones of pelvic ganglia (Nishimura *et al.* 1988), also eliminated the PTH, so that the PTD appeared

during repetitive firing of pelvic ganglia neurones. Removal of extracellular calcium inhibited PTD. The PTD was augmented in a low-chloride solution (Fig. 10*C*). These results suggest that substantial activation of $G_{Cl\text{-}Ca}$ (calcium-activated chloride conductance) occurs during repetitive firing of pelvic ganglia neurones.

DISCUSSION

The present results strongly suggest that neurones in rabbit parasympathetic ganglia have a calcium-dependent anion conductance. The properties of the anion current resemble those described in cultured neurones of rat DRG (Mayer, 1985; Scott *et al.* 1988), spinal cord from mice (Owen *et al.* 1984) and quail trigeminal ganglia (Bader *et al.* 1987). In cultured parasympathetic neurones taken from quail embryonic ciliary ganglia, there was no calcium-dependent chloride current ($I_{Cl\text{-}Ca}$) in most neurones tested (Bader *et al.* 1987). $I_{Cl\text{-}Ca}$ may not be expressed *in vivo* early in the development of quail parasympathetic ganglia as stated by Bader *et al.* (1987).

The activation mechanism of this anion conductance is similar to that described in *Xenopus* oocytes (Barish, 1983), cultured DRG neurones (Mayer, 1985) and pituitary cells (Korn & Weight, 1987). They reported that barium ions did not activate chloride current. Miledi & Parker (1984) also reported poor ability of barium ions compared to calcium ions to activate the divalent cation-dependent chloride conductance. On the other hand, Scott *et al.* (1988) have demonstrated the chloride tail current in barium-containing medium. From experiments using caffeine, they have suggested that barium does not directly activate the chloride tail current, but triggers release of intracellular calcium ions. Our present results showed that the tail current was strongly reduced by substitution of barium for calcium. In contrast to the poor ability of barium to activate the chloride tail current in neurones of pelvic ganglia, strontium appeared to produce the tail current. Selectivity of divalent cations for activation of chloride conductance or release of intracellular calcium from a calcium store site might be different in individual preparations.

Recent studies on various excitable membranes have suggested the occurrence of several calcium currents (Carbone & Lux, 1984; Bossu, Feltz & Thomann, 1985; Nowycky *et al.* 1985; Fox *et al.* 1987; Narahashi, Tsunoo & Yoshii, 1987; Kostyuk, Shuba & Savchenko, 1988). Our present results showed that the transient (T) type current could be evoked by a voltage jump from a holding potential of -100 to -50 mV in neurones of pelvic ganglia. When the membrane potential was held at -60 to -70 mV between voltage jumps, where the T-type calcium current is assumed to be inactivated (Nowycky *et al.* 1985; Fox *et al.* 1987), an ω-conotoxin-sensitive inward calcium current appeared to be evoked at -20 mV. An isolated L-type current was also recorded from neurones of pelvic ganglia by a voltage jump from -40 to -20 mV. $I_{Cl\text{-}Ca}$ could not be activated under conditions where the T-current was likely to be activated. In contrast, sustained (N- and L-type) calcium currents can activate a chloride current tail. Since the mean resting membrane potential of pelvic ganglia neurones ranged between -60 and -50 mV (Nishimura *et al.* 1988), the N-type and L-type calcium currents may be responsible for the generation of the chloride current under physiological conditions.

Our previous report together with the present results suggests that the membrane

of pelvic ganglia neurones is endowed with at least two calcium-dependent conductance systems, namely $G_{K\text{-}Ca}$ and $G_{Cl\text{-}Ca}$ (Nishimura *et al.* 1988; Tokimasa *et al.* 1988*a*, *b*; Nishimura, Tokimasa & Akasu, 1989). A single action potential was usually followed by a slow after-hyperpolarization (AHP) due to activation of a $G_{K\text{-}Ca}$ (Nishimura *et al.* 1988). However, a depolarizing after-potential (ADP) could also be recorded when potassium conductances were blocked by intracellular injection of caesium ions or extracellular application of tetraethylammonium. Persistent calcium influx during a prolonged calcium spike may activate calcium-dependent chloride channels (Tokimasa *et al.* 1988*a*). Our present results show that T-type currents were not responsible for generation of the tail current. The amplitude and decay time constant of the chloride tail current increase with the duration of the depolarizing pre-pulses used to trigger the sustained calcium currents. These results suggest that larger calcium entry may be needed for activation of chloride conductance rather than for potassium conductance. A slow rate of rise of the tail current can also be accounted for by the slow activation kinetics of $I_{Cl\ Ca}$.

It is well known that an increased calcium influx during repetitive action potentials causes a long-lasting activation of $G_{K\text{-}Ca}$, resulting in a generation of the post-tetanic hyperpolarization (PTH). Generally, the PTH lasts for a few minutes after termination of repetitive spikes in various autonomic neurones, because of a summation of the AHP (Minota, 1974; North, 1982). Although repetitive firing of pelvic ganglia neurones also produced the PTH, its duration was shorter than that of single-spike AHP. Furthermore, after a complete blockade of the AHP by curare or apamin a depolarizing after-potential, the post-tetanic depolarization (PTD), could be observed. The PTD was augmented by lowering external chloride concentration. Thus, a calcium-dependent chloride conductance can be activated during a burst of action potentials.

This work was supported by a Grant-in-Aid for Scientific Research from the Ministry of Education, Science and Culture of Japan. We would like to thank Professor Joel P. Gallagher for reading our manuscript.

REFERENCES

BADER, C. R., BERTRAND, D. & SCHLICHTER, R. (1987). Calcium-activated chloride current in cultured sensory and parasympathetic quail neurones. *Journal of Physiology* **394**, 125–148.

BARISH, M. E. (1983). A transient calcium-dependent chloride current in the immature *Xenopus* oocyte. *Journal of Physiology* **342**, 309–325.

BOSSU, J. L., FELTZ, A. & THOMANN, J. M. (1985). Depolarization elicits two distinct calcium currents in vertebrate sensory neurones. *Pflügers Archiv* **403**, 360–368.

BREHM, P. & ECKERT, R. (1978). Calcium entry leads to inactivation of calcium channel in *Paramecium*. *Science* **202**, 1203–1206.

BRETAG, A. H. (1987). Muscle chloride channels. *Physiological Reviews* **67**, 618–724.

CARBONE, E. & LUX, H. D. (1984). A low voltage-activated, fully inactivating Ca channel in vertebrate sensory neurones. *Nature* **301**, 501–502.

COLQUHOUN, D., NEHER, E., REUTER, H. & STEVENS, C. F. (1981). Inward current channels activated by intracellular Ca in cultured cardiac cells. *Nature* **294**, 752–754.

FOX, A. P., NOWYCKY, M. C. & TSIEN, R. W. (1987). Kinetic and pharmacological properties distinguishing three types of calcium currents in chick sensory neurones. *Journal of Physiology* **394**, 149–172.

GRAY, P. T. A. & RITCHIE, J. M. (1986). A voltage-gated chloride conductance in rat cultured astrocytes. *Proceedings of the Royal Society* B **228**, 267–288.

HILLE, B. (1984). *Ionic Channels of Excitable Membranes*. Sinauer Associates Inc., Sunderland, MA, USA.

INOUE, I. (1985). Voltage-dependent chloride conductance of the squid axon membrane and its blockade by some disulfonic stilbene derivatives. *Journal of General Physiology* **85**, 519–537.

KORN, S. J. & WEIGHT, F. F. (1987). Patch-clamp study of the calcium-dependent chloride current in AtT-20 pituitary cells. *Journal of Neurophysiology* **58**, 1431–1451.

KOSTYUK, P. G., SHUBA, YA. M. & SAVCHENKO, A. N. (1988). Three types of calcium channels in the membrane of mouse sensory neurons. *Pflügers Archiv* **411**, 661–669.

MCCLESKEY, E. W., FOX, A. P., FELDMAN, D. H., CRUZ, L. J., OLIVERA, B. M., TSIEN, R. W. & YOSHIKAMI, D. (1987). ω-Conotoxin: direct and persistent blockade of specific types of calcium channels in neurons but not muscle. *Proceedings of the National Academy of Sciences of the USA* **84**, 4327–4331.

MAYER, M. L. (1985). A calcium-activated chloride current generates the after-depolarization of rat sensory neurones in culture. *Journal of Physiology* **364**, 217–239.

MILEDI, R. & PARKER, I. (1984). Chloride current induced by injection of calcium into *Xenopus* oocytes. *Journal of Physiology* **357**, 173–183.

MINOTA, S. (1974). Calcium ions and the post-tetanic hyperpolarization of bullfrog sympathetic ganglion cells. *Japanese Journal of Physiology* **24**, 501–512.

NARAHASHI, T., TSUNOO, A. & YOSHII, M. (1987). Characterization of two types of calcium channels in mouse neuroblastoma cells. *Journal of Physiology* **383**, 231–249.

NISHIMURA, T., TOKIMASA, T. & AKASU, T. (1988). Calcium-dependent potassium conductance in neurons of rabbit vesical pelvic ganglia. *Journal of the Autonomic Nervous System* **24**, 133–145.

NISHIMURA, T., TOKIMASA, T. & AKASU, T. (1989). Voltage clamp analysis of calcium-sensitive chloride current ($I_{Cl\text{-}Ca}$) endowed on neuronal membrane in rabbit vesical pelvic ganglia. *Neuroscience Research*, suppl. 9, 75.

NORTH, R. A. (1982). Electrophysiology of the enteric nervous system. *Neuroscience* **7**, 315–325.

NOWYCKY, M. C., FOX, A. P. & TSIEN, R. W. (1985). Three types of neuronal calcium channel with different calcium agonist sensitivity. *Nature* **316**, 440–443.

OWEN, D. G., SEGAL, M. & BARKER, J. L. (1984). A Ca-dependent Cl^- conductance in cultured mouse spinal neurones. *Nature* **311**, 567–570.

PARTRIDGE, L. D. & SWANDULLA, D. (1988). Calcium-activated non-specific cation channels. *Trends in Neurosciences* **11**, 69–72.

ROGAWSKI, M. A., INOUE, K., SUZUKI, S. & BARKER, J. L. (1988). A slow calcium-dependent chloride conductance in clonal anterior pituitary cells. *Journal of Neurophysiology* **59**, 1854–1870.

SCOTT, R. H., MCGUIRK, S. M. & DOLPHIN, A. C. (1988). Modulation of divalent cation-activated chloride ion currents. *British Journal of Pharmacology* **94**, 653–662.

TILLOTSON, D. (1979). Inactivation of Ca conductance dependent on entry of Ca ions in molluscan neurons. *Proceedings of the National Academy of Sciences of the USA* **76**, 1497–1500.

TOKIMASA, T., NISHIMURA, T. & AKASU, T. (1988*a*). Calcium-activated chloride conductance in parasympathetic neurons of the rabbit urinary bladder. *Journal of the Autonomic Nervous System* **24**, 123–131.

TOKIMASA, T., NISHIMURA, T., TSURUSAKI, M. & AKASU, T. (1988*b*). Calcium-activated potassium and chloride currents in rabbit parasympathetic neurons. *Society for Neuroscience Abstracts* **14**, 946.